Mesoscopic Fluctuations of the Critical Current in a Superconductor–Normal-Conductor–Superconductor

Hideaki Takayanagi,[1] Jørn Bindslev Hansen,[2] and Junsaku Nitta[1]
[1] *NTT Basic Research Laboratories, 3-1, Morinosato-Wakamiya, Atsugi-shi, Kanagawa 243-01, Japan*
[2] *NKT Research Center, Sognevej 11, DK-2605 Brøndby, Denmark*
(Received 22 June 1994)

Mesoscopic fluctuations are observed for the critical current in a superconductor–normal-conductor–superconductor junction using the inversion layer of p-type InAs as the normal conductor. As a function of the gate voltage (i.e., the Fermi energy) the critical current and the conductance exhibit mesoscopic fluctuations in both the weak and the strong localization regimes. The magnitude and the typical period of the fluctuations are discussed and compared to theoretical predictions.

PACS numbers: 74.40.+k, 74.50.+r, 74.60.Jg

For several years there has been a growing interest in the way the mesoscopic phenomena may appear in the quantum transport of superconducting structures coupled with mesoscopic-scale normal metals or semiconductors [1]. In the ballistic regime of the normal conductor a superconducting quantum point contact (SQPC) was proposed [2,3]. In the dirty regime of the normal conductor Al'tshuler and Spivak have calculated the mesoscopic fluctuations of the critical current I_c in a superconductor–normal-conductor–superconductor (S-N-S) junction [4]. According to their theory, the I_c fluctuations are due to quantum interference effects. Beenakker has studied an S-N-S junction shorter than the coherence length and showed that the magnitude of the I_c fluctuation ΔI_c becomes universal [5]. Here $\Delta I_c \equiv \mathrm{rms} I_c = \sqrt{\langle I_c^2\rangle - \langle I_c\rangle^2}$. So far, none of these predictions have been confirmed experimentally.

There are two methods for observing mesoscopic fluctuations of the critical current as well as of the conductance G_N. There are measurements of I_c and G_N as a function of either a magnetic field or the Fermi energy E_F. The former method is difficult to use because of the well-known field sensitivity of the Josephson currents in a spatially extended S-N-S junction. The latter method is very effective for measurements of the I_c fluctuations provided that the carrier concentration of the normal conductor can be changed. A gated semiconductor-coupled Josephson junction is particularly suited for this purpose. In this Letter, we report on the experimental confirmation of the existence of mesoscopic I_c fluctuations by means of a p-type InAs coupled Josephson junction [6], and we compare the experimental results with theoretical predictions.

Figure 1 shows a schematic view of the sample geometry. Two superconducting Nb electrodes are coupled through the surface inversion layer on a p-type InAs substrate. Niobium was deposited at an angle up to a thickness of about 100 nm, and the Nb film on the channel was removed by lift-off technique. The junction has a metal-insulator-semiconductor gate. The gate insulator consists of a 70 nm thick anodic oxide film of InAs and a film of 100 nm of electron-beam deposited SiO. The gate structure could reproducibly withstand a gate voltage V_g of up to -20 V applied between the gate and one of the Nb electrodes. This gate configuration made it possible to vary the carrier concentration N_s (i.e., E_F) and mobility μ of the inversion layer by the gate voltage over 1 order of magnitude, and this resulted in a change of the critical current I_c and the normal resistance R_N of the junction over 3 orders of magnitude.

For the sample used in this study, the separation between the two Nb electrodes L was between 0.3 and 1 μm. In this range of L a supercurrent flows through the two-dimensional electron gas (2DEG) formed in the inversion layer and the junctions show dc and ac Josephson junction characteristics up to about 6 K [6].

In order to confirm the existence of mesoscopic I_c fluctuations we studied the reproducibility, i.e., the sample specific I_c fingerprints. Figure 2 shows measured I_c for a sample with $L = 0.4$ μm as a function of the gate voltage at $T \sim 20$ mK. The second series of measurements were made just after the first. During both series of measurements I_c was optimized by a small magnetic field ($\sim$0.1 G) applied perpendicular to the 2DEG. Over the range of

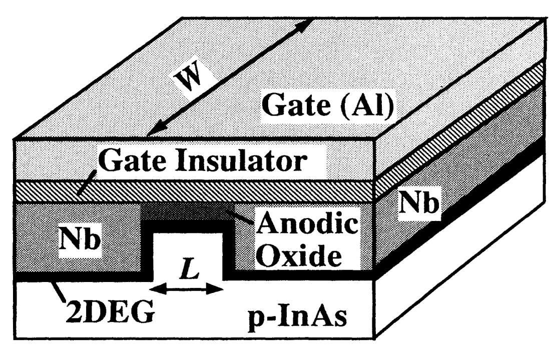

FIG. 1. A schematic cross sectional view of the Nb-2DEG-Nb junction geometry. The supercurrent flows through the two-dimensional electron gas (2DEG) formed in the inversion layer of the p-type InAs substrate. The conductance and the critical supercurrent are changed by the gate voltage.

 0031-9007/95/74(1)/166(4)$06.00

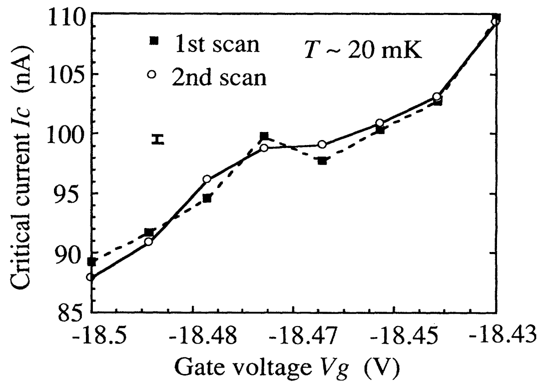

FIG. 2. The critical current measured as a function of the gate voltage. The second series of measurements were carried out just after the first one. The coincidence between the two data sets shows the reproducibility of the measurement of the critical current fluctuations with the gate voltage.

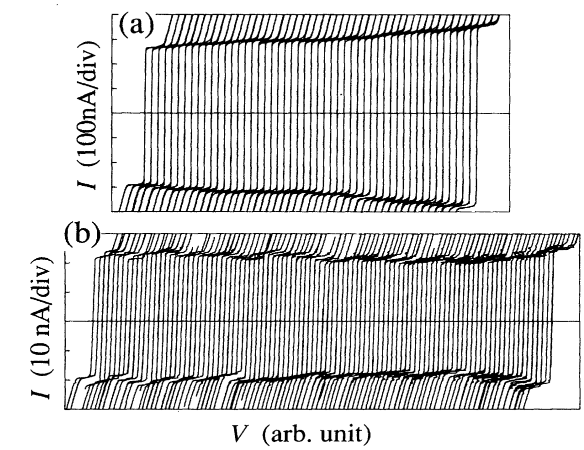

FIG. 3. All I-V curves measured for (a) $V_g = -15.9$ to 16.4 V and $T \sim 20$ mK (regime 1), and (b) $V_g = -19.0$ to 20.0 V and $T \sim 20$ mK (regime 2). The I-V curve is plotted every 10 mV gate voltage from right to left.

V_g shown in Fig. 2, the magnitude of the applied magnetic field which maximized I_c was constant. As shown, in both measurements I_c fluctuations were observed and the second measurement series showed satisfactory agreement with the first one. This proves that these I_c variations are not time-dependent noise but time-independent reproducible fluctuations within the sample.

Over a wide range of V_g from -15 to -20 V, we measured I_c for another sample with $L = 0.4$ μm at 20 mK very precisely. I_c showed fluctuations in all gate-voltage regimes. For this sample two typical regimes of V_g were selected to present our measurement of the mesoscopic fluctuations of I_c vs V_g. One is the range from -15.9 to -16.4 V (regime 1) and the other is from -19 to -20 V (regime 2). The selected gate-voltage regime is rather narrow, since almost constant R_N in the regime makes it possible to compare the experimental results with the theoretical predictions.

Figures 3(a) and 3(b) show current-voltage (I-V) curves measured at intervals of 10 mV in regimes 1 and 2, respectively. I_c was carefully optimized by applying a small magnetic field. In the range of V_g from -15 to -20 V, the magnitude of the magnetic field which maximized I_c changed gradually. However, over a narrow range of V_g like regimes 1 and 2 it was constant.

In regime 1, I_c was determined with an accuracy of about 3 nA from the I-V curve [see Fig. 3(a)]. At the same time the normal conductance G_n was also obtained from this curve, since it is difficult to measure I_c and R_N very accurately at the same time. G_n is defined here as $G_n = 1/R_n$, where R_n is the differential resistance measured for a bias current of 0.8 μA. R_n is not the same as R_N, however, R_n is proportional to R_N. G_n may be used to observe the normal conductance fluctuations. I_c and G_n as a function of V_g are shown in Fig. 4. As is clearly seen, both G_n and I_c show fluctuations as a function of V_g, i.e., with varying the Fermi energy. It is shown later that the physical origin of the measured G_n fluctuations is the same as that of universal conductance fluctuations (UCF). The behavior of the I_c curve tracks almost that of G_n. These indicate that the fluctuations of I_c have the same physical origin as that of UCF. From the data we find that the magnitude of I_c fluctuations ΔI_c is about 15 nA and the typical period V_p in V_g is about 80 mV.

Next, typical experimental results for regime 2 are shown. In regime 2, I_c was determined with an accuracy of about 0.3 nA. G_n is given as $G_n = 1/R_n$, where R_n is the differential resistance for a bias current of 40 nA. Using the data shown in Fig. 3(b), I_c and G_n as a function of V_g were obtained as shown in Fig. 5(a). In this case, the behavior of the I_c fluctuations very precisely follows that of the G_n fluctuations. It could be thought

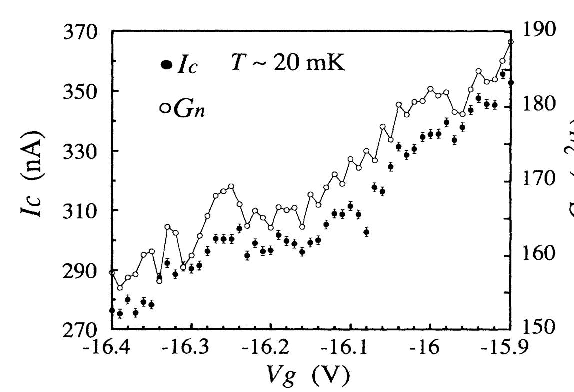

FIG. 4. The critical current I_c and the conductance G_n as a function of V_g in regime 1. The behavior of I_c tracks that of G_n.

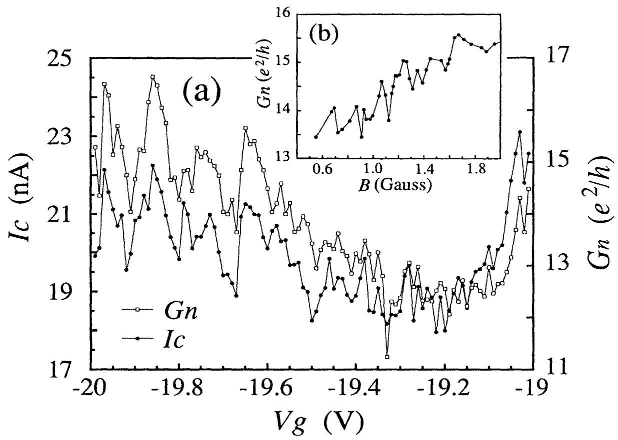

FIG. 5. (a) The critical current I_c and the conductance G_n as a function of V_g in regime 2. The behavior of I_c tracks precisely that of G_n. (b) G_n as a function of the magnetic field B for $V_g = -19.9$ V.

that the G_n fluctuations were due to the fluctuations in I_c, i.e., that the slope of the I-V curve would change with a change in I_c. In order to clarify this possible dependence we induced at $V_g = -19.9$ V a 10% reduction in I_c by changing the applied magnetic field very slightly. The resulting change in G_n was an increase of 0.06%. From such observations we may infer that G_n fluctuates independently of I_c.

To study the G_n fluctuations more closely, we measured G_n as a function of the magnetic field B for $T \sim 20$ mK and $V_g = -19.9$ V. The definition of G_n was the same as above. The result is shown in Fig. 5(b): The $G_n(B)$ fluctuations have a magnitude of $(1-1.5)e^2/h$ and a typical period of 0.2 G. We note that the magnitude of the $G_n(B)$ fluctuations is similar to the $G_n(V_g)$ fluctuations shown in Fig. 5(a). Because of flux focusing by the diamagnetic Nb thin film electrodes, the magnetic field in the 2DEG is enhanced over the applied field by a factor of up to $F_{\max} = (2W/L)^{2/3}$ [7]. The geometry used $F_{\max} = 54$. From the result shown in Figs. 5(a) and 5(b) we may infer that the G_n fluctuations as a function of the gate voltage and of the magnetic field both have the same origin as UCF. As will be discussed later, regime 2 belongs to the strongly localized regime. The good agreement between the I_c and the G_n fluctuations clearly demonstrates that the I_c fluctuations have the same origin as UCF in the strong localization regime. From measurements in this regime we obtained typically ΔI_c of 2–4 nA and V_p of about 100 mV.

In the following sections we will discuss the experimental data in relation to the theories by Al'tshuler and Spivak [4] and by Beenakker [5,10]. The system may be characterized by the following parameters: the coherence length ξ, the mean free path l, the correlation energy E_c, and the randomness parameter $\lambda = \hbar/2\pi E_F \tau = 1/k_F l$, where τ is the elastic scattering time and E_F and k_F are the Fermi energy and momentum, respectively. These parameters are calculated as follows: (1) The key transport parameter for the 2DEG, the diffusion constant D, is found from R_N using the relations $D = em^*/\pi\hbar^2 N_s \mu$ and $N_s \mu = L/eWR_N$; here m^* is the effective mass, N_s the carrier concentration, and μ the mobility of the 2DEG. W is the junction width. For the junction considered $W = 80$ μm and $m^* = 0.024 m_e$ (m_e is the free electron mass). By using R_N values at 4 K where the localization effect may be neglected we find for the two regimes: regime 1, $D = 2.1 \times 10^{-3}$ m^2/s ($R_N = 150$ Ω), and regime 2, $D = 6.2 \times 10^{-4}$ m^2/s ($R_N = 500$ Ω). (2) In the dirty limit $\xi = (\xi_0 l)^{1/2}$, where $\xi_0 = \hbar v_F/\pi\Delta_0$ (v_F is the Fermi velocity of the 2DEG). In terms of D, $\xi = (2\hbar D/\pi\Delta_0)^{1/2}$. (3) l is found from N_s and μ: $l = \hbar\mu(2\pi N_s)^{1/2}/e$. From the $N_s\mu$ product and Yamaguchi's data for $N_s(\mu)$ at 4.2 K [9], N_s and μ are roughly evaluated, and l at $T \sim 4$ K found for both regimes. (4) $E_c = \hbar\pi^2 D/L^2$ is also obtained from D [8]. (5) Finally, also from D, we find $\lambda = \hbar/2\pi D m^*$ (λ is the expansion parameter in the weakly localized regime). For the two regimes the values of these parameters are shown in Table I. Except for $k_B T$ the values are for $T \sim 4$ K. They do not show any strong temperature dependence down to $T \sim 20$ mK.

From Table I it is clear that for both regimes $E_c > k_B T$ is satisfied, and therefore mesoscopic fluctuations may be observed in both regimes. We also see that L exceeds ξ and l. From the λ values we conclude that regime 1 is at the limit of the region where weak localization theory may be adopted, while regime 2 belongs to the strongly localized regime. We are now, finally, able to compare the experimental results with theoretical predictions. Al'tshuler and Spivak [4] found, for $L \gg \xi$, $T \ll T_N$ ($\equiv \hbar D/2k_B L^2$), and $L \ll W, L_z$:

$$\Delta I_c \approx \frac{eE_c}{h}\left\{\frac{15\zeta(5)}{\pi}\frac{WL_z}{L^2}\right\}^{1/2}, \tag{1}$$

TABLE I. Characteristic lengths and energies for both regimes.

	L (μm)	W (μm)	ξ (nm)	l (nm)	D (m^2/s)	E_c (eV)	$k_B T$ ($T \approx 20$ mK) (eV)	λ
Regime 1	0.4	80	20	8	2.1×10^{-3}	8.5×10^{-5}	1.7×10^{-6}	0.37
Regime 2	0.4	80	10	2	6.2×10^{-4}	2.5×10^{-5}	1.7×10^{-6}	1.2

which in our 2D case reduces to

$$\Delta I_c \approx 2.2 \frac{eD}{L^2} \left\{ \frac{W}{L} \right\}^{1/2} . \quad (2)$$

Here $\zeta(x)$ is the Riemann zeta function and L_z is the thickness of the 3D normal conductor. For $L \ll \xi$, Beenakker calculated ΔI_c and showed that for $T \ll T_c$ ΔI_c depends only on the gap of the superconductor Δ_0: $\Delta I_c \approx 0.3 e\Delta_0/\hbar$ [5,10]. For Nb $T_c \sim 9$ K and $\Delta I_c = 0.11$ μA.

In both regimes our experimental data nearly satisfy the conditions for Al'tshuler and Spivak's condition but not for Beenakker's. Using Eq. (2) the theoretical value for ΔI_c for regimes 1 and 2, respectively, are 65 and 20 nA, while the experimental values are $\sim$15 nA and $2 \sim 4$ nA. We note that at $T \sim 20$ mK the condition $T \ll T_N = \hbar D/2k_B L^2$ is only marginally satisfied for the two regimes for which $T_N = 50$ and 15 mK are found. This is a possible reason for the reduction of the experimental ΔI_c. There are at least two other effects we know which will suppress ΔI_c: (1) Andreev reflection at the SN interfaces [11] and (2) Coulomb interaction associated with Anderson localization [12]. Moreover, it was observed that at low temperatures I_c for junctions with the same structure decreased with decreasing temperature [13]. This effect may also reduce I_c.

With respect to the fluctuations observed in the $G_n(B)$ data [Fig. 5(b)], we note that the typical period is given by $B_c \sim h/eWL$ [8]. For the junction considered here $B_c \sim 1.3$ G is about 6.5 times the observed period of 0.2 G, a discrepancy which we can account for by the flux focusing effect discussed above.

Finally, we will discuss the typical period V_p of the fluctuations in the $I_c(V_g)$ and $G_n(V_g)$ curves. V_p is given as $V_p = E_c/\alpha$, $\alpha = dE_F/dV_g$, where

$$\alpha = \frac{\pi\hbar^2}{m^*}\frac{dN_s}{dV_g} = \frac{L}{eW}\left[\frac{dR_N^{-1}}{dV_g} \bigg/ \left(N_s \frac{d\mu}{dN_s} + \mu\right)\right]. \quad (3)$$

dR_N^{-1}/dV_g is determined experimentally and $d\mu/dN_s$ is evaluated from Ref. [9]. Theoretical V_p values of 30 and 60 mV are found for regimes 1 and 2, respectively, in good agreement with the experimental values from the $I_c(V_g)$ data: $V_p = 80$ and 100 mV. This agreement indicates that the mesoscopic fluctuations of I_c and G_n are due to the change in the Fermi energy.

In summary, the mesoscopic fluctuations of the critical current in an S-N-S junction were confirmed experimentally by means of a p-type InAs coupled Josephson junction with a gate structure. The observed magnitude of the critical current fluctuations was smaller than the theoretical predictions. This discrepancy was discussed based on the fact that the measurement temperature ($\sim$20 mK) was still high for the measured carrier concentration and that Andreev reflection as well as Coulomb interaction affected the magnitude of the fluctuation. The typical period of the fluctuations with the gate voltage and with a magnetic field was also studied, and it was found that the experimental results agreed reasonably well with the calculated values.

Our experimental data give clear evidence of the mesoscopic fluctuations of the critical current and show that the interference effects as well as Coulomb interaction play an important role in the superconducting transport in an S-N-S junction at low temperatures.

The authors would like to thank Professor H. Fukuyama, Dr. B. J. van Wees, Dr. Y. Takane, Dr. H. Yoshioka, Dr. A. Furusaki, and Dr. H. Nakano for their useful discussions of mesoscopic fluctuations. One of the authors (H. T.) is indebted to Professor C. W. J. Beenakker for stimulating him to this study. They also wish to thank Dr. T. Kimura and Dr. H. Hiratsuka for their encouragement throughout this work.

[1] T. M. Klapwijk, Physica (Amsterdam) **197B**, 481 (1994).
[2] C. W. J. Beenakker and H. van Houten, Phys. Rev. Lett. **66**, 3056 (1991).
[3] A. Furusaki, H. Takayanagi, and M. Tsukada, Phys. Rev. Lett. **67**, 132 (1991); Phys. Rev. B **45**, 10 563 (1992).
[4] B. L. Al'tshuler and B. Z. Spivak, Zh. Eksp. Teor. Fiz. **92**, 609 (1987) [Sov. Phys. JETP **65**, 343 (1987)].
[5] C. W. J. Beenakker, Phys. Rev. Lett. **67**, 3836 (1991); **68**, 1442(E) (1992).
[6] H. Takayanagi and T. Kawakami, Phys. Rev. Lett. **54**, 2449 (1985).
[7] J. Gu, W. Cha, K. Gamo, and S. Numba, J. Appl. Phys. **50**, 6437 (1979).
[8] E. Yamaguchi, Phys. Rev. B **32**, 5280 (1985).
[9] P. A. Lee, A. D. Stone, and H. Fukuyama, Phys. Rev. B **35**, 1039 (1987).
[10] C. W. J. Beenakker and B. Rejaei, Phys. Rev. B **49**, 7499 (1994).
[11] A. F. Andreev, Zh. Eksp. Teor. Fiz. **46**, 1823 (1964) [Sov. Phys. JETP **19**, 1228 (1964)].
[12] H. Fukuyama and S. Maekawa, J. Phys. Soc. Jpn. **55**, 1814 (1986).
[13] H. Takayanagi, J. B. Hansen, and J. Nitta (unpublished).